

Effect of various focusing schemes of ultrasound on stone erosion rate using cavitation bubbles

様々な集束超音波によるキャビテーション気泡を用いた結石破碎速度への影響

Toshiya Yura^{1†}, Maxime Lafond², Shin Yoshizawa¹, and Shin-ichiro Umemura²
(¹School of Eng., Tohoku Univ., ²School of Biomed. Eng., Tohoku Univ.)

由良俊哉^{1†}, ラフォンマキシム², 吉澤晋¹, 梅村晋一郎²(¹東北大院 工,²東北大院 医工)

1. Introduction

Shock Wave Lithotripsy (SWL) has been one of the several first-line treatments for crushing kidney stones¹. However, SWL has two problems. Firstly, it can damage to normal tissue surrounding kidney stone, being caused by cavitation. Secondly, it tends to produce residual stone fragments too large to path through the ureters, which have also been reported².

High-intensity focused ultrasound (HIFU) is a noninvasive treatment method in which the ultrasound energy is generated outside the body and focused on the target in tissue³. In the focal region, intense negative pressure may lead to the formation and oscillation of micrometrical bubbles: acoustic cavitation. This phenomenon is known to cause erosion and kidney stones can be fragmented into small pieces⁴. For the comminution of kidney stones by HIFU, high intensity pulses are used to repeatedly generate cavitation bubbles. However, the stone erosion rate by this method is significantly lower than conventional treatment method SWL.

The control of cavitation bubble behavior is important because at a high intensity and pulse repetition frequency (PRF), a large cavitation cloud can act as a shield protecting the calculi to be efficiently eroded. To optimize the cavitation in the focal region and to improve stone erosion rate, various focal geometries are created by a phased array transducer and their effect on the rate and behavior of erosion rate are investigated.

2. Materials and Methods

2.1 Experimental Setup

Fig. 1 shows a schematic of the experimental setup. A 128-channel array spherical transducer with a geometrical focal length of 120 mm was settled in an acrylic tank containing degassed water. The geometric focus of the transducer was located on the surface of a model stone made from cement powder and tap water mixed at the stoichiometric ratio of 5:1 (g:g). The Vickers hardness of the stones was measured with a

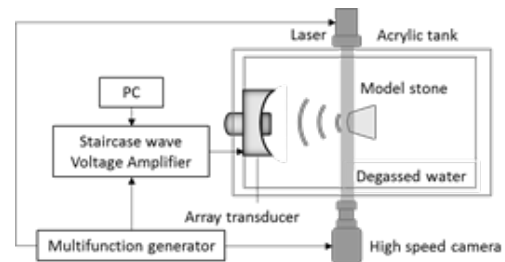


Fig. 1 Schematic of experimental setup

50 g load to be 95.9 ± 20.1 , which is consistent with the previous measurements of the natural and model stones⁵. The length of a diagonal line through the center was 13 mm and the height was 13 mm as well. A high speed camera was settled at the side of the tank to observe cavitation behavior on the surface of the stones.

2.2 Split Focus method

The transducer has 128-channel elements that are driven at a frequency of 1 MHz individually. Therefore each element can be driven at different phases to shape various foci. The phase of each element to form a sector vortex foci are given as^{6,7}

$$\theta = m \frac{i2\pi}{N} \quad i = 1, 2, \dots, N \quad (1)$$

where N : sector number, m : vortex mode

Especially, when $N=2m$, a “Split Focus” is formed. **Fig. 2** shows the pressure fields of Single Focus ($m=0$) at left and Split Focus ($N=4, m=2$) at middle on focal plane. They are normalized by each maximum value. In the Split Focus, the focal region is laterally split into 4 sub-foci. In contrast, the even harmonic components are still focused at the

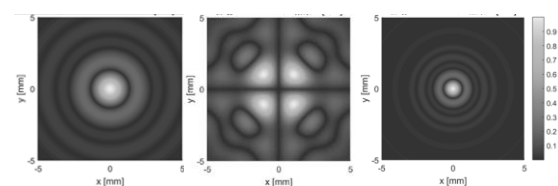


Fig. 2 Focal shape in Split Focus

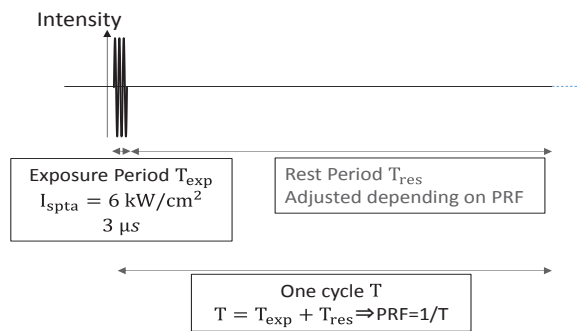


Fig. 3 Schematic of ultrasound sequence

geometrical focal point, as shown in the right figure of **Fig. 2**. Therefore, Split Focus may have two advantages: 1) a wider focal region, and 2) less nonlinear effect on reducing the negative focal pressure.

2.3 Waveform and Sequence

The sequence of HIFU exposure in the experiment is shown in **Fig. 3**. The exposure time of HIFU was $3 \mu\text{s}$. The intensity was 60 kW/cm^2 at geometrical focal point for Single Focus exposure. It was compared with Split Focus exposure at the same focal acoustic power. The repetition frequency (PRF) of the sequence was varied by adjusting the intermission period between each consecutive sequences. The sequence was repeated for 1 min at a PRF of 1, 5, 10 and 20 kHz and for 2 min at a PRF of only 0.1 kHz.

3. Results and discussion

3.1 High-speed optical images and Residual fragmented stones

High speed optical images on the surface of model stones without and with exposure of the Single Focus and Split Focus are shown in **Fig. 4**. With Single Focus, cavitation bubbles were induced from the surface of model stones to the transducer⁸. However, with Split Focus, cavitation bubbles were generated only on the surface of stones more thinly and more widely than with Single Focus as expected.

Partly fragmented stones after ultrasound exposure at a PRF of 10 kHz are shown in the **Fig. 5**. The left is the stone fragmented by Single Focus, and that by Split Focus in the right. Fragmentation by Split Focus was contiguous rather

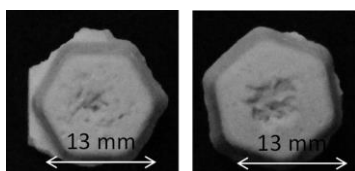


Fig. 5 Partly fragmented stones after exposure

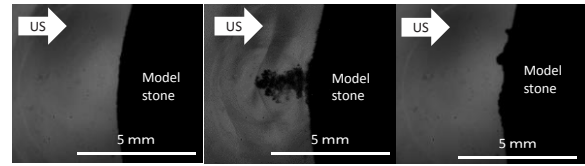


Fig. 4 High speed images without exposure and with exposure of Single Focus and Split Focus

than separated into 4, which was the number of sub-foci. It is thought that the stone was fragmented even by the cavitation bubbles induced by the second harmonic component at geometrical focal point.

4. Conclusion

In this study, the behavior of cavitation bubbles on the surface of model stones in the focal region of HIFU with various focusing schemes were observed with a high speed camera optically. The surfaces of the partly fragmented stones were also observed. With Split Focus, cavitation bubbles were induced only on the surface of the stone more thinly and more widely than Single Focus, and a contiguous fragmented region was formed. It is expected that Split Focus scheme will provide a more efficient method of fragmenting stones than the conventional Single Focus.

References

1. O. A. Sapozhnikov, A. D. Maxwell, B. MacConaghy, and M. R. Bailey: *J Acoust Soc Am*, Vol.121, No.2, pp.1190-1202, February (2007)
2. A. P. Duryea, A. D. Maxwell, W. W. Roberts, Z. Xu, T. L. Hall, C. A. Cain: *IEEE Trans Ultrason Ferroelectr Freq Control*, Vol.58, No.5, pp.971-980, (2011)
3. S. Yoshizawa, T. Ikeda, A. Ito, R. Ota, S. Takagi, Y. Matsumoto: *Med Biol Eng Comput*, Vol.47, No.8, pp.851-860, (2009)
4. T. Ikeda, S. Yoshizawa, M. Tosaki, et al.: *Ultrasound in Med. & Biol.* Vol. 32, No.9, pp.1383-1397, (2006)
5. D. Heimbach, R. Munver, P. Zhong, et al.: *The Journal of Urology*. Vol.164, No.2, pp.537-544, (2000)
6. S. Umemura and C. A. Cain: *IEEE Trans Ferroelectrics Freq Contr*, Vol.39, No.1, pp.32-38, (1992)
7. C. A. Cain, S. Umemura: *IEEE Trans Microw Theor Tech*, Vol.34, No.5, pp.542-550, (1986)
8. A. D. Maxwell, T. Wang, C. A. Cain, et al.: *J. Acoust. Soc. Am.* Vol.130, No.4, pp.1888-1898, (2011)